Experimental Evaluation and Modeling of a Regenerative Braking System for an Electric Motorcycle

Nguyen Van Tinh*, Huynh Thuan Phat, Dang Quoc Cuong

Nguyen Tat Thanh University, Ho Chi Minh City, Viet Nam
*nvtinh@ntt.edu.vn

Abstract

This research presents an experimental evaluation, modeling and simulation of a regenerative braking system for an electric motorcycle based on the VinFast Klara S platform equipped with a 1.2 kW brushless direct current motor. An experimental test bench was established to examine the effects of battery state of charge and braking power on energy recovery efficiency. The results indicate that the maximum recovery efficiency reached 22.5% at a braking power of 200 W, within an optimal state of charge range of (50-60)%. A Matlab/Simulink model was developed and validated using experimental data to assess the impact of the RBS on the motorcycle's driving range. Under the proposed urban driving cycle, the driving range per full charge increased from 63.64 km to 67.06 km, corresponding to an improvement of 5.4%. The study also clarified the influence of the rectifier-boost converter efficiency, battery internal resistance and proposed directions to enhance the performance of regenerative braking systems for small electric motorcycles.

Received 13/03/2026
Accepted 07/04/2026
Published 28/04/2026

Keywords

RBS system; EM; energy recovery; simulation; efficiency.

1 Introduction

In recent years, electric vehicles (Evs) have been considered as one of the efficient means to decrease greenhouse gas emissions and to improve energy efficiency of the transportation sector. Electric powertrain efficiency and environmental effects have been studied in numerous studies in the context of on road urban mobility [1]. One of the major constraints of EVs is the restricted driving range which depends heavily on the battery capacity and the energy management strategy. Regenerative braking system (RBS) have been widely used in electric and hybrid electric vehicles to utilize electric energy efficiently. RBS enables the recovery of a portion of the vehicle's kinetic energy during braking and converts it into electrical energy stored in the battery of the vehicle [2]. Therefore, RBS have been reported to help increasing the vehicle's energy efficiency and extending the driving range which is highly beneficial for urban driving conditions as they involve large amounts of braking and acceleration [3].

At present, most studies on RBS are concentrated on EVs and hybrid electric vehicles (HEVs), where sophisticated control algorithms and power electronics are designed to enhance the conversion of braking energy via the traction motor [4]. Intelligent braking control and motor control strategies for enhancing the

https://doi.org/10.55401/rc15zm17

braking torque and stability of the entire vehicle during RBS have also been studied [5]. In recent years, RBS technology has been increasingly focused on application in light-weight vehicles such as electric motorcycles and electric bikes. A few modeling and simulation techniques have been proposed to study the implications of RBS on vehicle performance and battery state of charge (SOC) [6, 7]. These results suggest that the energy efficiency of such vehicles can be improved via regen braking. However, the realistic efficiency of braking energy recovery is generally limited by losses in power electronics processing and limitations related to batteries performance. There are few studies on RBSs specifically designed for electric motorcycles (EMs), and most of the research is concentrated on simulation or conceptual design without experimental validation [8, 9]. Hence, integrated studies combining experimental testing and simulation modeling for EMs are still necessary.

This study was initiated to address the lack of RBS in the literature for Vietnamese EVs. We introduce an analytical RBS for the VinFast Klara S electric motorcycle (EM) powered by a brushless direct current (BLDC) hub motor. This study investigated the performance of the RBS for the motorcycle test with the identified parameters implemented in Matlab/Simulink.

2 Theoretical Background

2.1 Operating principle of the RBS

EMs have a drivetrain system that converts the electrical energy from the battery to initiate movement, basically into a mechanical force that turns the wheels of the motorcycle. Among various types of motors applied, BLDC motor is the most common type of motor used in EMs due to several advantages, including light-weight design and high energy efficiency. However, the BLDC motor still has several limitations that may affect its suitability for use in EM operation [10].

In traction mode, a permanent magnet BLDC motor acts as the prime mover. The throttle signals are received by the controller, and it controls the battery current flow using a DC-AC inverter and feeds the three-phase currents to the stator windings. These currents produce a rotating magnetic field, which interacts with the rotor magnets to produce torque; and back electromotive force (EMF) is used to detect rotor position and perform correct commutation.

In decelerating or braking operation (regenerative mode), the BLDC motor acts as a generator. As a result of inertia, the rotor is turned due to the weight of the motorcycle and induce an EMF in the stator windings, which creates a regenerative current. This current is fed back into the battery converting some of the motorcycle's kinetic energy into electrical energy. The electromagnetic torque also acts to slow down the motorcycle, assisting with the deceleration process.

2.2 Selection of base motorcycle

Several major manufacturers are currently active in the Vietnamese EM market, including VinFast, Pega, and Yadea. Among them, VinFast leads the market with the largest share in recent years, as reported by the International Council on Clean Transportation (ICCT) [11]. In this study, VinFast Klara S is used as a representative platform to develop and evaluate a RBS. Its technical specifications are mainly employed for model calibration and driving cycle development, ensuring realistic operating conditions.

Table 1 The VinFast Klara S EM's technical parameters [13]

Motor Type	12 inch BLDC
Rated Power/Peak power (w)	1,200 / 1,700
Battery Type	Lithium 22 Ah 60 V
Full Charging Time (h)	3 h (90% SOC) or 4,8 h (100% SOC) per battery
Max Speed (km/h)	48
Load Capacity (kg)	150
Motorcycle and Battery Mass (kg)	108

The objective is not to replicate the original motocycle configuration, but to assess the effectiveness of RBS in terms of energy recovery and driving range improvement. Therefore, while a 1.2 kW BLDC motor is retained, a 60 V/20 Ah lead-acid battery was adopted. This choice reflected the widespread use of lead-acid

batteries in low-cost electric motorcycles, which typically lack RBS. Thus, the study focuses on evaluating the practical benefits of RBS for this vehicle category. The differences between lithium-ion and lead-acid batteries, particularly in terms of internal resistance and charge-discharge behavior, are acknowledged as a limitation and will be addressed in future work.

2.3 Development of driving cycle

Furthermore, the motorcycle speed can be different by changing the velocity input signal. This input was random and depended entirely on the rider's will, according to the driving cycle. From this, the total resistive force at a given speed defined by the cycle can be obtained (F_{Load})($V_{demand(t)}$). A PI control algorithm was then applied to regulate the actual motor speed ($V_{act(t)}$). Consequently, the simulation yielded the final outcomes, namely the demanded power (P_{k_demand}) and the demanded traction force (F_{k_demand}) as functions of time-varying motorcycle speed.

$$F_{demand}(t) = F_c(t) + F_{PI}(t) \quad (1)$$

$$F_c(t) = F_f(t) + F_w(t) + F_j(t) \quad (2)$$

$$F_{PI}(t) = K_p e(t) + K_i \int_0^t e(\tau) \quad (3)$$

$$e(t) = V_{demand}(t) - V_{act}(t) \quad (4)$$

$$P_{demand}(t) = F_{demand}(t) \times V_{demand}(t) \quad (5)$$

A dedicated test cycle must be developed specifically for EMs in Viet Nam to objectively assess the effectiveness of RBS during simulation. Standard test cycles such as ECE-R40 and Japan 10-Mode are commonly used for urban performance simulations of passenger motorcycles. However, these cycles are not suitable for the Klara S model, which has a rated power of only 1,200 W (1,700 W peak) and falls under the EM category according to regulation for motorcycles with motor power below 4 kW [12]. In addition, the maximum speed of the VinFast Klara is limited to 48 km/h (see Table 1)

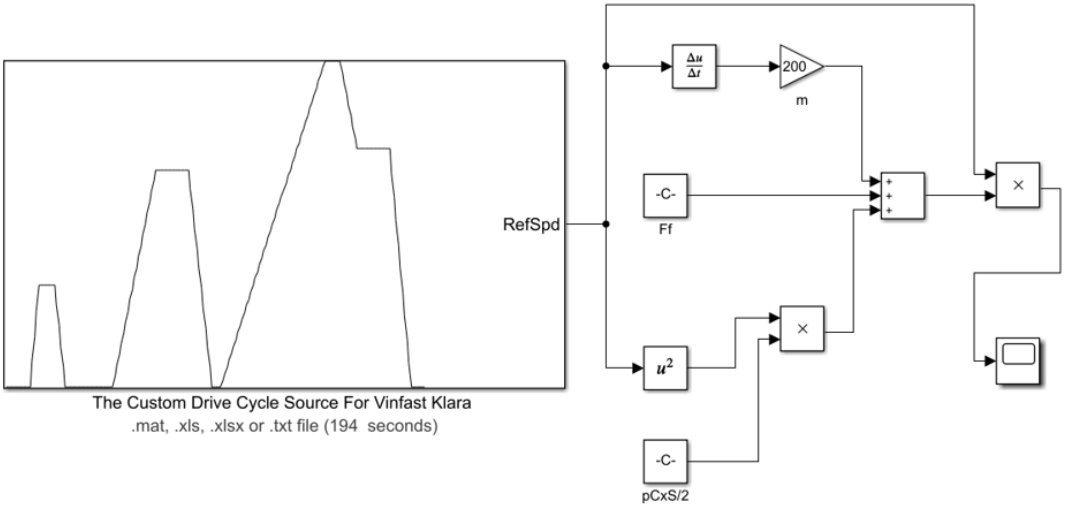

Figure 1 Dynamic model of EM movement

In this research, based on the technical parameters shown in Table 1, a motorcycle dynamics model was built by using Matlab/Simulink. A corresponding test cycle that suits the operating ability of the motorcycle was selected while keeping the traction requirement below the peak power of the motor. The simulation analyses the performance of the motorcycle in terms of traction force, which is determined by the balance of traction and resistance forces through motorcycle dynamics equations.

$$F_f + F_w \pm F_j \pm F_i \le F_k \le F_{k\max} \quad (6)$$

The quantities F_f, F_w, F_j, and F_i represent the rolling resistance, aerodynamic drag, inertial resistance, and gradient resistance, respectively. In this study, it was assumed that the motorcycle operated on flat roads within urban areas; thus, the gradient resistance was

neglected, and only rolling resistance, aerodynamic drag, and inertial resistance were considered.

$$F_f = G \times f = m \times g \times f \quad (7)$$

$$F_W = \frac{1}{2} \times C_d \times A \times \rho \times V^2 \quad (8)$$

$$F_{max} = m \times j_{max} \quad (9)$$

Once the total resistive forces were determined, they were combined with motorcycle velocity to obtain the required traction power according to the following equation:

$$P_k \geq P_c = F_c \times V \quad (10)$$

A motorcycle dynamics simulation model was developed to examine the suitability of the proposed test cycle. In this model, the resistive force components were represented as separate functional blocks, thereby enabling an accurate assessment of the cycle's required power and verifying its feasibility according to equation. Simulation results in Figure 2 showed that the maximum traction power was about 1,589 W, below the motor peak power of 1,700 W. Therefore, the test cycle is appropriate.

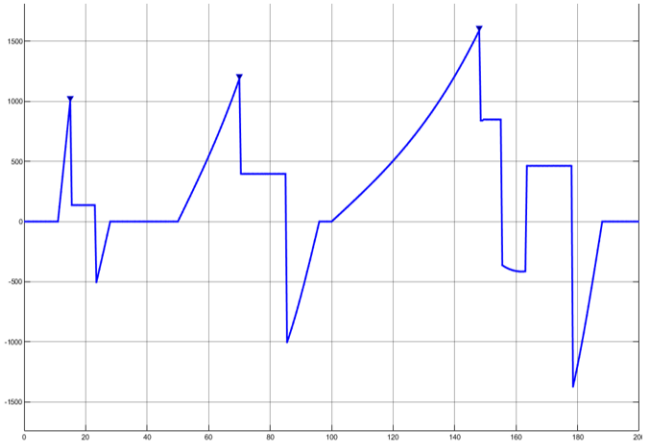

Figure 2 Motorcycle power demand during the adjusted driving cycle

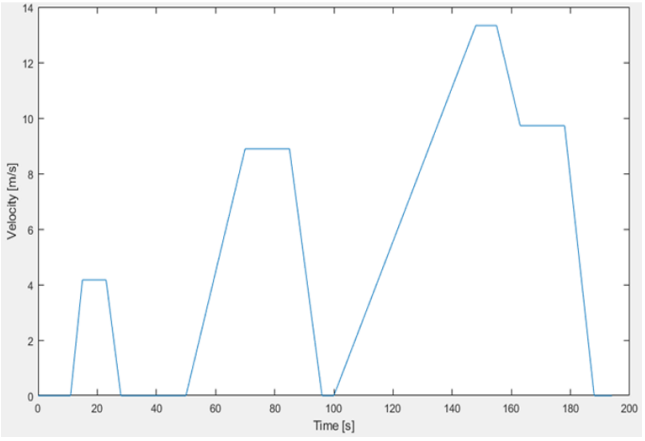

Figure 3 Adjusted driving cycle based on the ECE-R40 standard

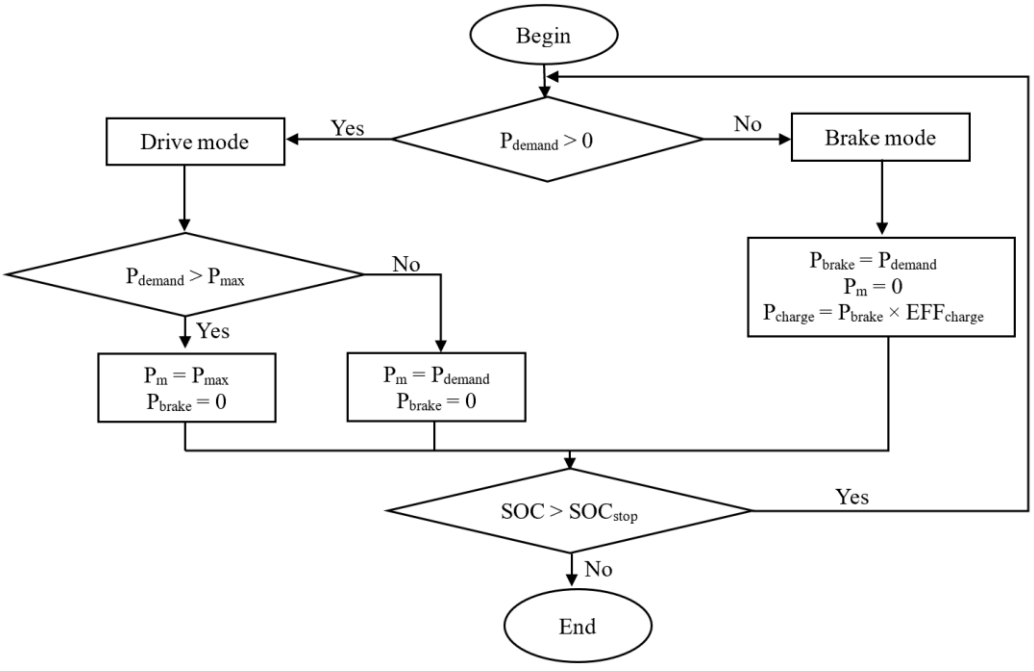

Figure 4 Control algorithm flowchart for traction and RBS modes

2.4 Modeling of power source

In an EM powertrain, the battery is the main energy source. Its output voltage varies with operating conditions, particularly charge/discharge current and temperature, which directly affects its ability to supply voltage and current.

$$SOC(t) = SOC_0 - \frac{1}{3600}\int_{t_0}^{t} \frac{I(\tau) \times \eta_{batt}}{Q_i} \quad (11)$$

$$SOC(t) = SOC_0 \quad (12)$$

The simulation is in line with the control algorithm flowchart as depicted in Figure 4. The demanded power from the driving cycle (P_{k_demand}) was used to decide whether the motorcycle ran in drive mode or brake mode. The controller power managed the power distribution to the hub motor and constrained the traction power to the permissible amount. In regeneration, charging power to battery was distributed and corresponding electric power (P_{elec}) was calculated during RBS.

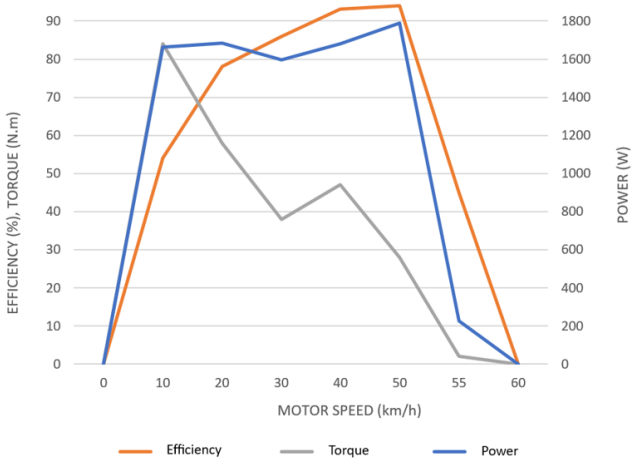

Figure 5 Hub motor 12-inch 1200W characteristic curve versus speed [14]

In the traction mode ($P_{k\_demand} > 0$), the braking power (P_{brake}) was set to zero, and the BLDC motor power demand (P_{m_demand}) equaled P_{k_demand}, but it was always constrained not to exceed the maximum motor power (P_{m_max}). In each operating mode, the motor power was associated with corresponding efficiency (η_m). Based on the Hub motor characteristic curve shown in Figure 5, the required input power for the Hub motor was determined.

$$P_{elec} = \frac{P_m}{\eta_m} \quad (13)$$

In the braking mode ($P_{k\_demand} < 0$), corresponding to the deceleration phases of the cycle, the BLDC motor operated as a generator and initiated the regenerative current recovery process. In this case, $P_{m\_demand} = 0$ and $P_{brake} = P_{k\_demand}$. The charging power (P_{charge}) was then supplied back to the battery pack. In practice, RBS in EMs did not function entirely independently but was typically combined with a mechanical braking system. However, in this study, the model was simplified to consider only the RBS in order to evaluate the system's effectiveness. By conducting experimental measurements on the RBS model, the charging recovery efficiency (EFF_Charge) was determined at SOC of 50%, 70%, and 90% for a 60 V/20 Ah lead-acid battery pack. Combined with the P_{brake}, the recovered charging power was calculated according to the following equation:

$$\boldsymbol{P_{elec} = P_{charge} = P_{brake} \times EFF_{Charge}} \quad (14)$$

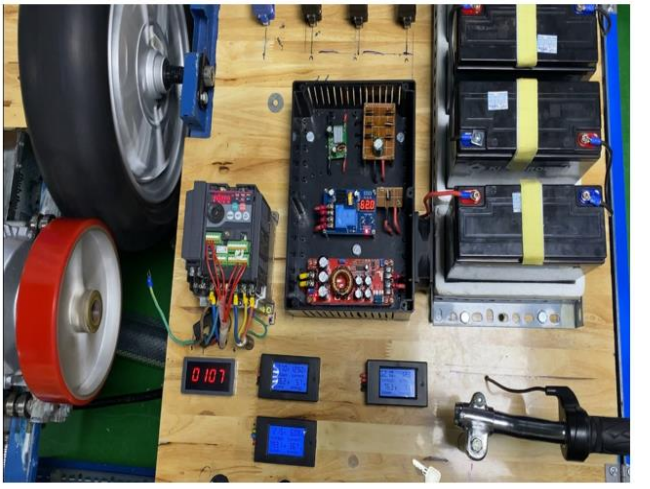

Figure 6 Operation of the RBS test bench for experimental measurement of regenerative current recovery efficiency

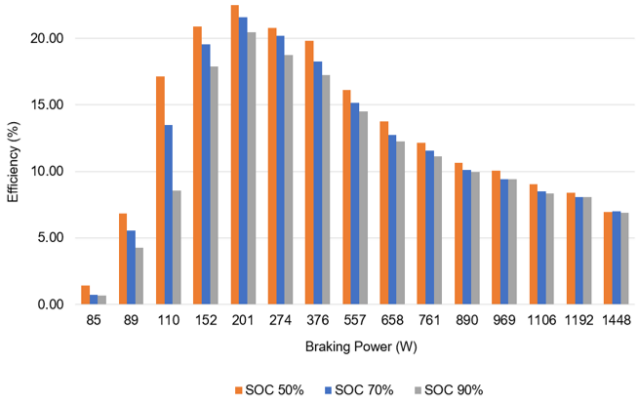

Figure 7 RBS recovery efficiency at different SOC levels after the boost circuit

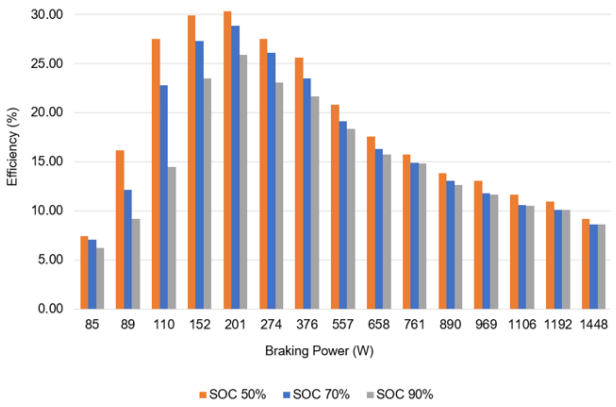

Figure 8 RBS recovery efficiency at different SOC levels before the boost circuit

To model the voltage characteristics of the battery pack, a simplified equivalent circuit model was commonly employed. In this model, the battery was represented as an ideal voltage source with an open-circuit voltage (U_{OC}), connected in series with an internal resistance that accounted for inherent losses. When a charging or discharging current flows through the battery, this internal resistance caused a voltage drop (U_r). Accordingly, the actual high-voltage output of the battery pack (U_{HV}) was determined by the following equation:

$$U_{HV} = U_{OC} - U_r \qquad (15)$$

The value of U_{OC} was modeled as a nonlinear function of SOC, which is typically determined through experimental measurements or approximation methods.

$$U_{OC} = f(SOC) \qquad (16)$$

The internal resistance of the battery varied depending on the operating temperature, SOC, and whether the battery was in charging or discharging mode. The voltage drops caused by internal resistance were determined according to Ohm's law:

$$U_r = i \times r \qquad (17)$$

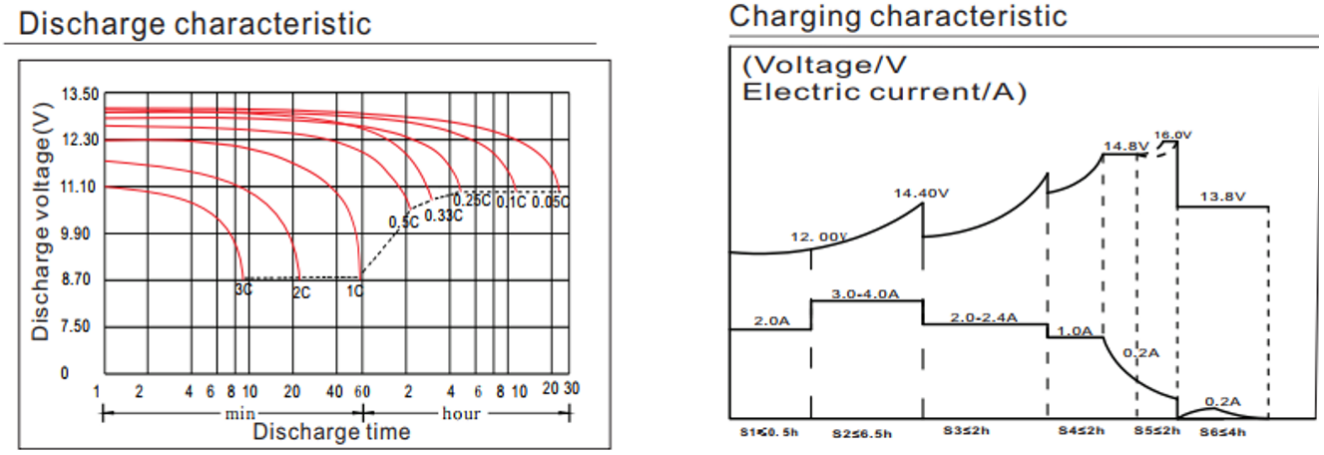

Figure 9 Characteristic curve of 6-DZF-20L lead-acid battery [15]

This model provided a simple yet effective approach to simulate the behavior of the battery pack under real operating conditions such as acceleration, deceleration, RBS or operation in varying temperature environments. Its application also supported the design process and the evaluation of energy efficiency, as well as the prediction of the battery pack's durability throughout its lifecycle.

3 Results and Discussion

The complete model was constructed using functional blocks of the EM in Matlab/Simulink. The simulation was carried out with the input velocity obtained from the driving cycle shown in Figure 3 as a function of time *t*. Battery SOC should remain above 50% to prevent damage and prolong its lifespan. Therefore, in the simulation, SOC_{stop} = 0.5 was used as the stop condition; the driving cycle terminated when SOC reached 0.5.

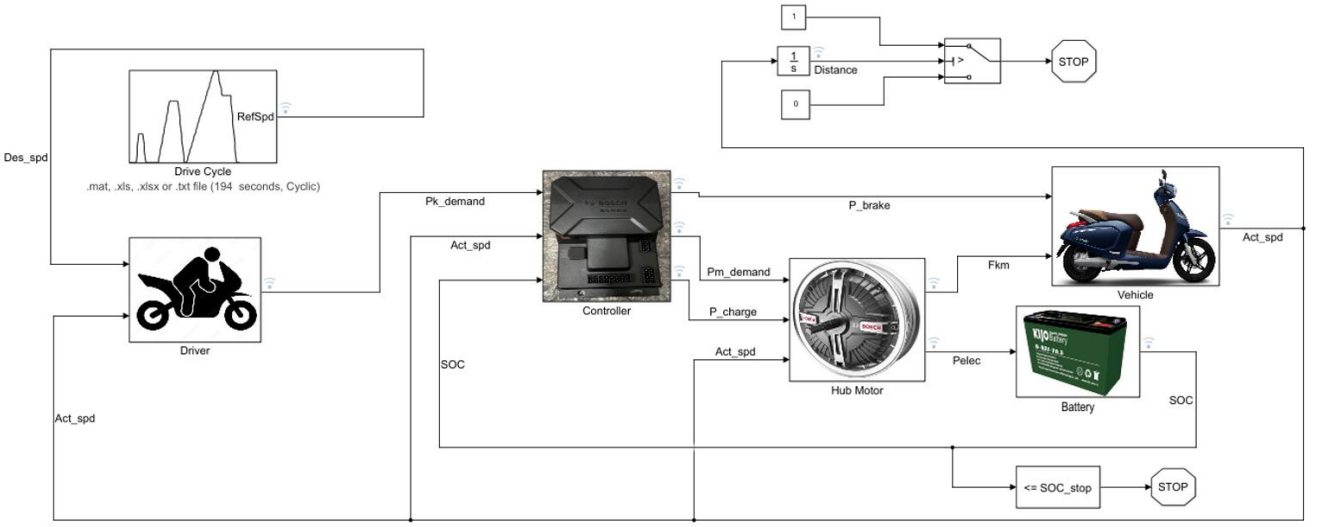

Figure 10 The model of the EM was simulated in Matlab/Simulink

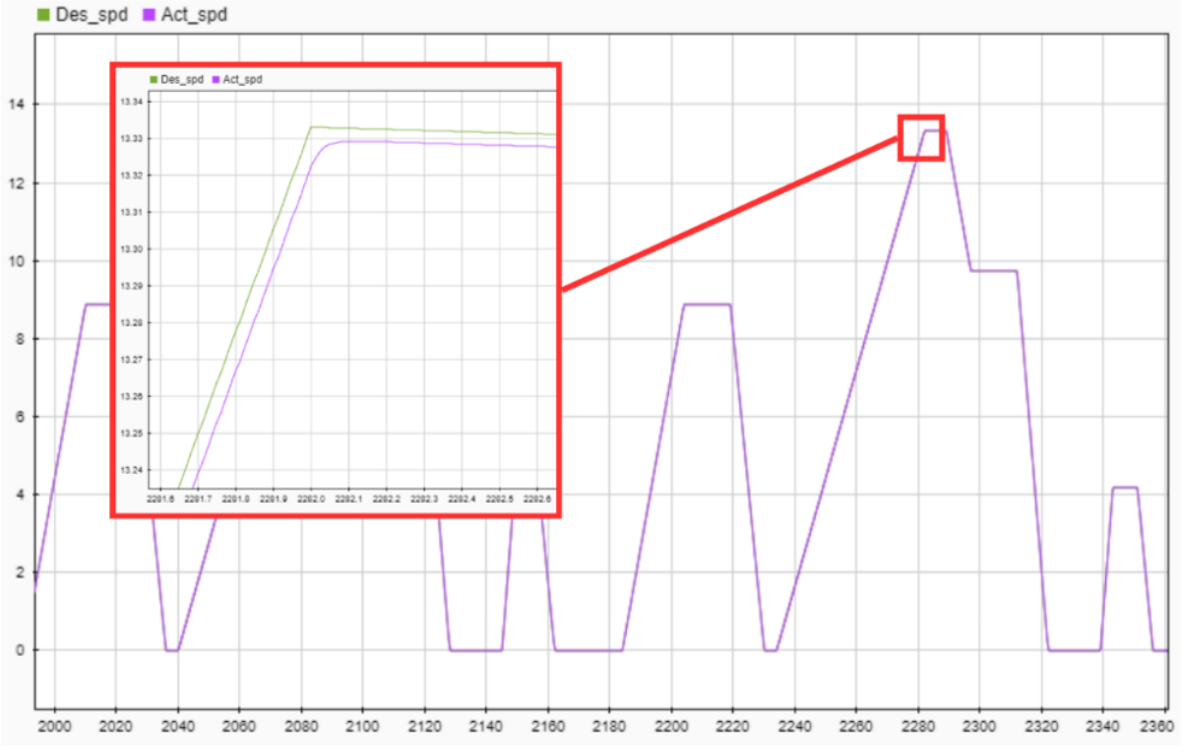

Figure 11 Result of simulation for response of PI algorithm at EM speed

Figure 11 showed the comparison of actual speed with the command speed in simulation. It can be seen that the difference was very small, indicating that the PI controller can stably and effectively control the motor speed. Yet, a lagged system response was observed, in particular at high vehicular speed (48 km/h). The error

is largely due to the application of a plain linear PI control without any special consideration on fast transient response. But the real speed gradually converged and held at the reference after the transient, which means that the system can keep good control accuracy under steady state, and the errors were too small to be taken into consideration.

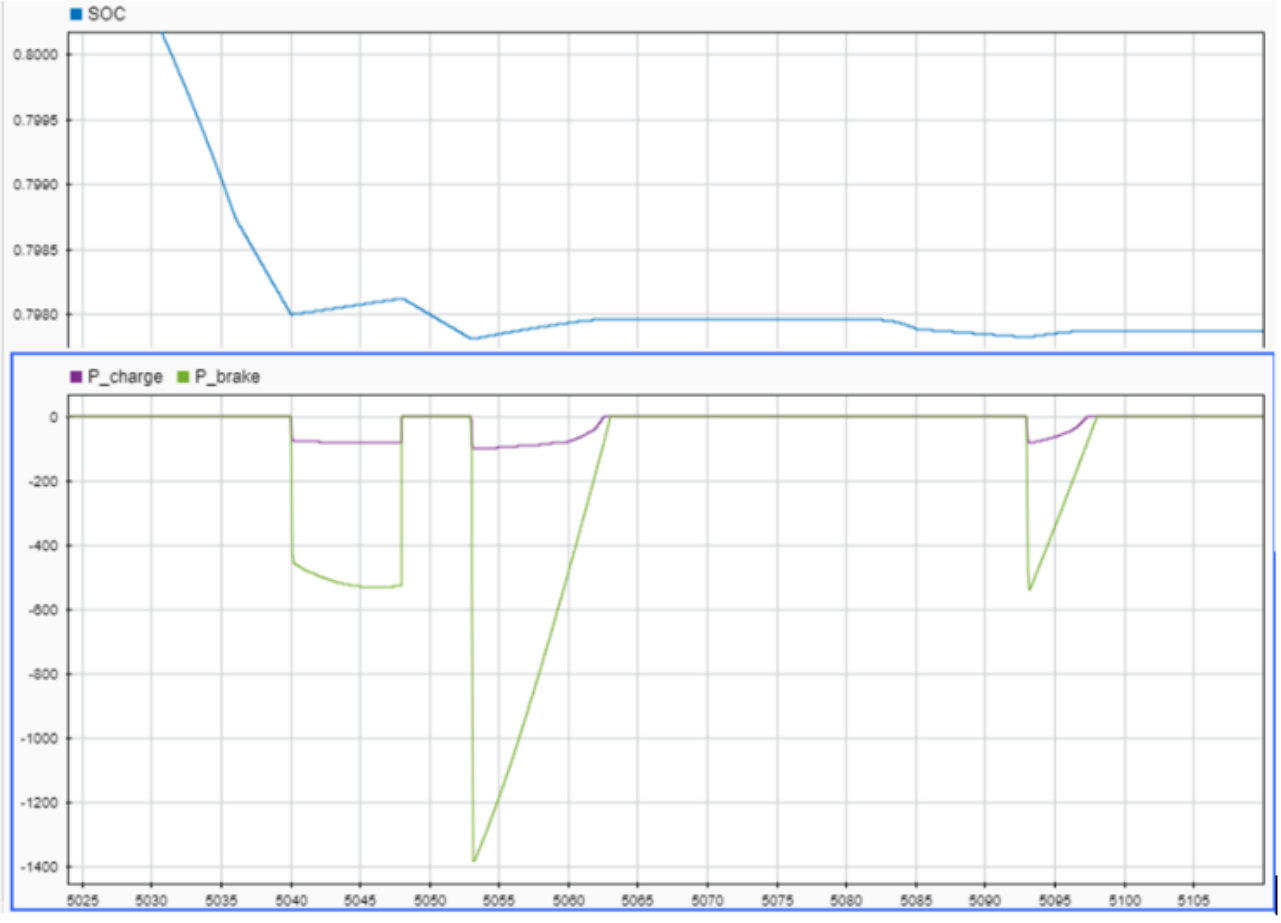

Figure 12 RBS energy recovery by decelerating with 60 V/20 Ah lead-acid battery

Figure 12 illustrates the change in SOC during brake. The SOC increased when P_{charge} was recovered via RBS by returning energy to the battery, and this is how the system regained braking energy.

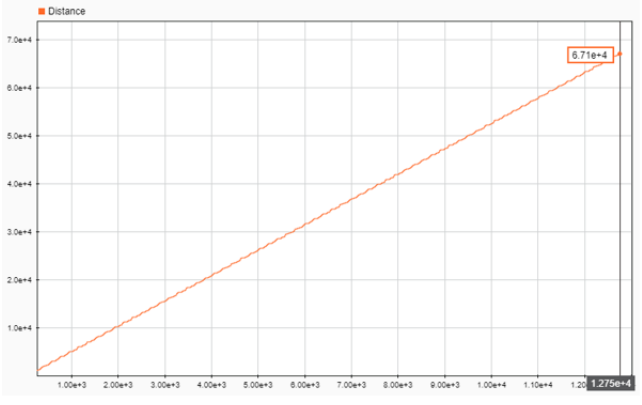

Figure 13 Driving range of motorcycles with RBS at SOC_{stop} limit 50%

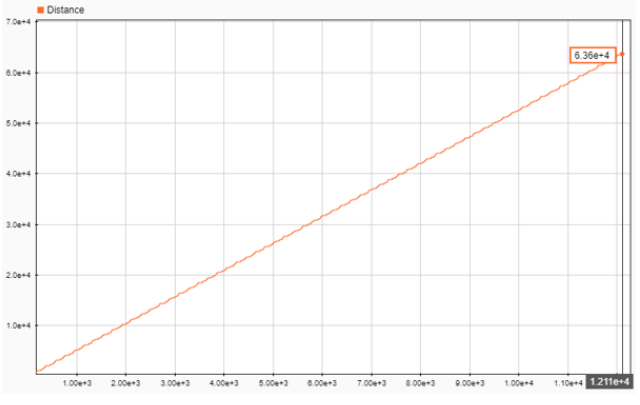

Figure 14 Driving range of the motorcycle without RBS at SOC_{stop} limit = 50%

Figure 13 and Figure 14 demonstrated the vehicle distance travelled in the simulation cycle with and without RBS, respectively. The ranges of motorcycles with RBS were 67.06 km and 63.64 km respectively, corresponding to an improvement of 5.4% in driving range. The extra simulations were run for different battery discharge limits, with SOC_{stop} = 50%, 60%, and 70%. Ideal and practical energy recovery efficiencies (Figure 7 and Figure 8) have been considered in the analysis.

Table 2 Driving range simulation at various operating conditions of VinFast Klara S powers by 60 V/20 Ah lead-acid battery

Driving Range (Km)	**SOC_{stop} 70%**	**SOC_{stop} 60%**	**SOC_{stop} 50%**
Ideal Recovery Efficiency	41.01	54.69	68.09
With RBS	40.44	53.81	67.06
Without RBS	38.47	51.1	63.64

As shown in Table 2, the travel distance achieved under the test cycle varies according to the battery discharge limit and the efficiency of the energy recovery system. At SOC_{stop} = 60%, the distance of motorcycle travel with regenerative braking was 54.69 km, while without RBS was 51.1 km, which led to an improvement of 7.02%. Nonetheless, because of the efficiency of the regenerative energy recovery device, which converted the generated AC during braking into DC and feeds the battery, the total benefit was still rather small.

4 Conclusion

This research presents an experimental investigation combined with simulation of an RBS for an electric motorcycle based on the VinFast Klara S platform using Matlab/Simulink. The results demonstrate that the RBS can recover a portion of the motorcycle's kinetic energy during braking. The recovery efficiency was influenced by the battery SOC and braking power, reaching a maximum value of approximately 22.5%. The integration of the RBS led to an increase in the driving range of about 5.4%, indicating its potential for application in low-power electric motorcycles.

The findings also indicated that the energy recovery performance is constrained by the efficiency of the rectifier-boost converter and the relatively high internal resistance of the lead-acid battery. Future work will focus on the implementation of high-efficiency power electronic converters and lithium-ion batteries, as well as real-world testing to further improve energy recovery capability and overall system reliability.

References

1. Firmansyah, D., Irawan, M. Z., Amrozi, M. R. F., Maitra, B., Rahman, T., & Widiastuti, N. O. (2024). A bibliometric analysis of motorcycle studies in Asia: From 1971 to 2022. *IATSS Research, 48*(1), 68-83.

2. Bhandari, P., Dubey, S., Kandu, S., & Deshbhratar, R. (2017). RBS systems: A review. *International Journal of Scientific & Engineering Research, 8*(2), 71-74.

3. Kropiwnicki, J., & Furmanek, M. (2019). Analysis of the regenerative braking system process for urban traffic conditions. *Combustion Engines, 178*, 203-207.

4. Nian, N. X., Peng, F., & Zhang, H. (2014). Regenerative braking system of electric vehicle driven by brushless DC motor. *IEEE Transactions on Industrial Electronics, 61*(10), 5798-5808.

5. Castillo Aguilar, J. J., Perez Fernandez, J., Velasco Garcia, J. M., & Cabrera Carrillo, J. A. (2017). Regenerative intelligent brake control for EMs. *Energies, 10*(10), Article 1648.

6. Worsfold, J., Anoh, K., Okafor, K. C., & Lipscomb, I. (2024). RBS in electric bicycles with supercapacitors for sustainable transport. In *Proceedings of the IEEE PES/IAS PowerAfrica Conference* (pp.1-5).

7. Corti, F., et al. (2024). Simulink-based simulation of electric bicycle dynamics and regenerative braking system for battery state of charge assessment. In *Proceedings of the IEEE Mediterranean Electrotechnical Conference (MELECON)* (pp. 803-808).
8. Huỳnh Thịnh, Nguyễn Văn Tình, Trần Cao Cường, Phạm Tuấn Anh, Nguyễn Văn Trạng. (2019). Study on hybrid technology integration for Honda Lead 110cc with regenerative braking system. *Proceedings of the Industrial Automation and Communications Project, Ho Chi Minh City University of Transport*.
9. Huynh Thuan Phat, Nguyen Hoang Viet, Nguyen Van Tinh (2026). Electric Motorcycles as a Sustainable Transportation Solution: The Potential of Regenerative Braking Systems in Vietnam. *Journal of Science and Development Economics*, No. 1(2026).
10. Mohanraj, D., et al. (2022). A review of BLDC motor: State of the art, advanced control techniques, and applications. *IEEE Access, 10*, 54833-54869.
11. International Council on Clean Transportation (ICCT). (2025). Vietnam two-wheelers market report. Washington, DC, USA.
12. Ministry of Transport of Vietnam. (2013). *QCVN 68:2013/BGTVT - National technical regulation on EMs and mopeds*.
13. VinFast. (2021). *Technical specifications of VinFast Klara S EM* (in Vietnamese). VinFast. https://vinfastauto.com/vn_vi/thong-so-ky-thuat-xe-may-dien-vinfast-klara-s
14.QS Motor. (2020). *Specifications of QS 12-inch 1200 W hub wheel motor* (Internal document).
15. Jiangxi Jingjiu Power Science & Technology Co., Ltd. (2024). *6-DZF-20L (6.10 kg) - Electric vehicle battery expert*. https://www.kijo-battery.com/uploads/file/6-dzf-20l-6.10kg-electric-vehicle-battery-expert.pdf

Đánh giá thực nghiệm và mô hình hóa hệ thống phanh tái sinh cho xe máy điện

Nguyễn Văn Tình*, Huỳnh Thuận Phát, Đặng Quốc Cường
Trường Đại học Nguyễn Tất Thành, Thành phố Hồ Chí Minh, Việt Nam
*nvtinh@ntt.edu.vn

Tóm tắt Nghiên cứu này trình bày việc đánh giá thực nghiệm, mô hình hóa và mô phỏng hệ thống phanh tái sinh cho xe máy điện dựa trên nền tảng VinFast Klara S sử dụng động cơ điện một chiều không chổi than 1,2 kW. Một mô hình thử nghiệm được xây dựng để đánh giá ảnh hưởng của trạng thái sạc pin và công suất phanh đến hiệu suất thu hồi năng lượng. Kết quả cho thấy hiệu suất thu hồi cực đại đạt 22,5 % tại công suất phanh 200 W, trong vùng SOC tối ưu (50-60)%. Mô hình Matlab/Simulink được phát triển và kiểm chứng bằng dữ liệu thực nghiệm nhằm đánh giá ảnh hưởng của hệ thống phanh tái sinh đến quãng đường di chuyển. Trong chu trình lái đô thị được xây dựng, quãng đường di chuyển trong một lần sạc đầy tăng từ 63,64 km lên 67,06 km, tương ứng cải thiện 5,4 %. Nghiên cứu làm rõ ảnh hưởng của hiệu suất bộ chỉnh lưu-khuếch đại điện áp và điện trở trong của pin, đồng thời đề xuất hướng nâng cao hiệu quả hệ thống phanh tái sinh cho xe máy điện cỡ nhỏ.

Từ khóa Phanh tái sinh; xe máy điện; thu hồi năng lượng; mô phỏng; hiệu suất.